Nanocrystalline-to-amorphous transition in nanolaminates grown by low temperature atomic layer deposition and related mechanical properties

R. Raghavan, Mikhael Bechelany, M. Parlinska, D. Frey, W. Mook, A. Beyer, J. Michler, I. Utke

Nanocrystalline-to-amorphous transition in nanolaminates grown by low temperature atomic layer deposition and related mechanical properties

R. Raghavan,[1] M. Bechelany,[2] M. Parlinska,[3] D. Frey,[1] W. M. Mook,[1,a)] A. Beyer,[4] J. Michler,[1] and I. Utke[1,b)]

[1]*EMPA, Swiss Federal Laboratories for Materials Science and Technology, Laboratory for Mechanics of Materials and Nanostructures, Feuerwerkerstrasse 39, CH-3602 Thun, Switzerland*
[2]*Institut Européen des Membranes (IEM/ ENSCM UM2 CNRS UMR 5635), Université Montpellier 2, Place Eugène Bataillon, 34095 Montpellier, France*
[3]*EMPA, Swiss Federal Laboratories for Materials Science and Technology, Electron Microscopy Center, Ueberlandstr. 129, CH-8600 Dübendorf, Switzerland*
[4]*University of Bielefeld, Faculty of Physics, Universitätsstrasse 25, D-33615 Bielefeld, Germany*

We report on a comprehensive structural and nanoindentation study of nanolaminates of Al_2O_3 and ZnO synthesized by atomic layer deposition (ALD). By reducing the bilayer thickness from 50 nm to below 1 nm, the nanocrystal size could be controlled in the nanolaminate structure. The softer and more compliant response of the multilayers as compared to the single layers of Al_2O_3 and ZnO is attributed to the structural change from nanocrystalline to amorphous at smaller bilayer thicknesses. It is also shown that ALD is a unique technique for studying the inverse Hall-Petch softening mechanism (E. Voce and D. Tabor, J. Inst. Metals **79**(12), 465 (1951)) related to grain size effects in nanomaterials. © *2012 American Institute of Physics*. [http://dx.doi.org/10.1063/1.4711767]

Atomic layer deposition (ALD) is an excellent technique to grow pinhole free, continuous, smooth, and substrate conformal thin films with precise dimensional control at the sub-nanometer level.[1,2] The self-limiting surface reactions involved during ALD promote the growth of precise multi-layered thin films on the substrate.[3] The high quality and substrate conformity of films deposited by ALD enables synthesis and surface engineering of complex nanostructures.[2,4] Moreover, low-temperature ALD (LT-ALD) within the range of 25–80 °C allows deposition on temperature-sensitive biological templates[5] and flexible polymer substrates[2,6,7] as well as on temperature sensitive metal oxide surfaces such as Cu_2O[8] thus opening the route to photovoltaic and energy-storage devices with innovative architectures.[9] In this article, we concentrate on the study of the transition from nanocrystalline to amorphous phases in thin nanolaminates of ZnO/Al_2O_3 grown by ALD at 65 °C and their related mechanical properties, hardness and Young's modulus.

The mechanical behavior of layered and nanocrystalline bulk materials has been a topic of extensive investigation. Several experimental studies have shown that polycrystalline and epitaxial multilayered thin films can be harder than their constituent components.[10] High hardness effects were also observed for nanocomposites[11] and for amorphous metal nanolaminates.[12] We report on softening of nanolaminates as a function of the bilayer thickness. This opens a route to tailor mechanical properties of (transparent conductive) oxide films for specific applications where mechanical integrity and reliability for opti-mum electrical and optical performance[13] is of utmost importance during service. We also address fundamental aspects of the nanolaminates' mechanical response to indentation at a nanoscale structural level.

In this study, seven different bilayer thicknesses of Al_2O_3/ZnO nanolaminates were investigated ranging from 48 nm to below 1 nm. Single layers of the constituent oxide compounds were investigated as reference. For experimental details on synthesis and characterization, see the supplementary information, Section S3.[20] Bilayer thicknesses of the nanolaminates are summarized in Table I together with individual thicknesses of the interlayers and the growth rate per cycle.

The growth rates of Al_2O_3 and ZnO in the nanolaminates vary between 1.4 to 2 Å per cycle and 1.8 to 2 Å per cycle, respectively. Multilayer stacks smaller than 0.9 nm Al_2O_3/1.6 nm ZnO (bilayer thickness 2.5 nm) were not measurable on cross sections by scanning He-ion microscopy due to resolution limits. Bilayer thicknesses of 1.3 nm and 0.8 nm represent extrapolated values based on the number of cycles and measured film thicknesses. Rutherford backscattering spectrometry (RBS) analysis on 100 nm thick single ZnO and Al_2O_3 films grown at 65 °C by ALD showed that the oxide compounds were stoichiometric. Elastic recoil detection analysis (ERDA) on Al_2O_3 showed a small hydrogen content around 6 at. %, which could be attributed to a partially hydroxylated phase AlO(OH).[7,14] The existence of such a phase is supported by mass spectrometry measurements performed on our nanolaminates showing the existence of an AlH^+ fragment in the Al_2O_3 multilayers.[15] However, transmission electron microscopy (TEM) observations did not show diffraction rings of phases other than ZnO.

Two illustrative examples of nanolaminates with bilayers thicknesses of 48 nm and 4.8 nm are shown in

---

a)Present address: Los Alamos National Laboratory, MPA-CINT, Center for Integrated Nanotechnologies, Los Alamos, New Mexico 87545, USA
b)Author to whom correspondence should be addressed. Electronic mail: ivo.utke@empa.ch.

TABLE I. Summary of low-temperature (65 °C) ALD Al_2O_3/ZnO nanolaminate experiments. Exposure cycles, total number of bilayers, resulting thicknesses for the film, the Al_2O_3 and ZnO interlayers, and the bilayers are reported.

| Cycles Al_2O_3 | Cycles ZnO | Number of Bilayers | Film Thickness (nm) | Interlayer Thickness (nm)/Growth per Cycle (Å) | | Bilayer Thickness (nm) |
				Al_2O_3	ZnO	
2	2	400	321	n.m.	n.m.	0.8[a]
4	3	200	271	n.m.	n.m.	1.3[a]
8	5	100	249	1.6/1.9	0.9/1.7	2.5
16	10	50	239	2.9/1.8	1.9/1.9	4.8
38	25	20	246	7.8/2.0	4.4/1.8	12.3
77	50	10	248	15.2/2.0	9.5/1.8	24.7
154	100	5	242	28.3/1.8	20.0/2.0	48.3
1540	—	0	223	1.4	—	single
—	1000	0	200	—	2.0	single

[a]Note that the bilayer thicknesses of 0.8 nm and 1.3 nm represent extrapolated values, which could not be verified by scanning electron/ion microscopy ("n.m." stands for not measurable).

Figures 1(a) and 1(b). The high-resolution secondary electron images of cross-sections of the nanolaminates were obtained by breaking the samples prior to observation in a He$^+$ ion microscope. More cross sectional images of the Al_2O_3/ZnO nanolaminates are shown in Figure S1[20] and confirm that the sequence of alternating Al_2O_3 and ZnO interlayers in the nanolaminate was achieved throughout the total film thickness down to a bilayer thickness of
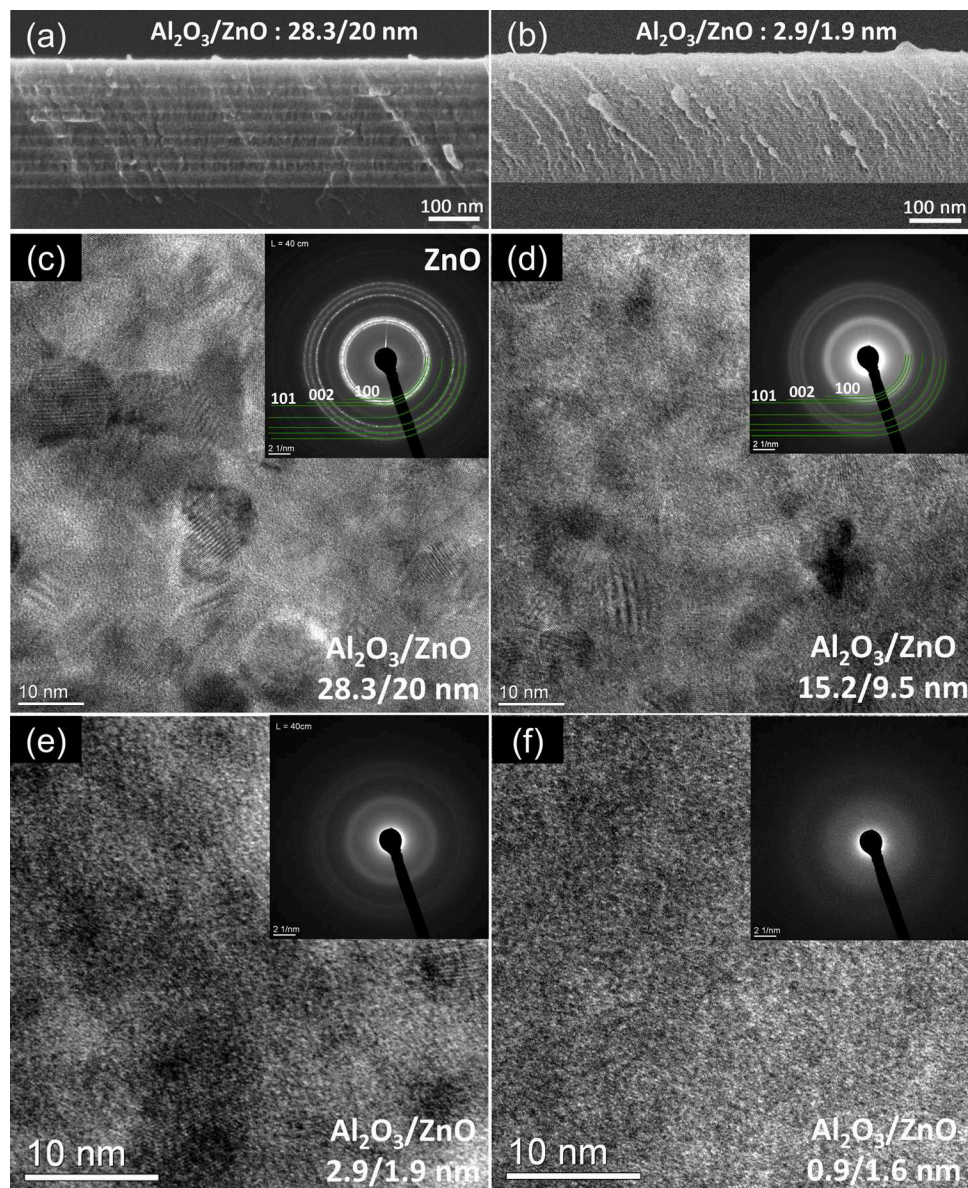

FIG. 1. Secondary electron images from a He-ion microscope of nanolaminate cross-sections with bilayer thicknesses of (a) 48.3 nm and (b) 4.8 nm. HRTEM images and electron diffraction patterns (insets) of nanolaminate films with bilayer thickness of (c) 48.3 nm, (d) 24.7 nm, (e) 4.8 nm, and (f) 2.5 nm. The diffraction pattern of the 48.3 nm thick bilayer nanolaminate can be exactly indexed to ZnO; for smaller bilayer thicknesses, the diffraction pattern fade out indicating amorphous ZnO deposition.

2.5 nm. Observation of smaller bilayer thicknesses was limited by the resolution of the scanning electron microscope or the He-FIB (focused ion beam) microscope, and the values presented in Table I were obtained by extrapolation. For all nanolaminates, the interface with the (111) Si substrate is Al_2O_3, while ZnO is the final film surface material. From a structural point of view, the nanolaminates of ZnO/Al_2O_3 studied in this article constitute alternating layers of amorphous Al_2O_3 and nanocrystalline ZnO as can be seen in high resolution transmission electron microscopy (HRTEM) images and electron diffraction patterns in Figures 1(c)–1(e). No Al_2O_3 diffraction rings were observed for any bilayer thickness, i.e., the Al_2O_3 deposited by ALD at 65 °C was amorphous in nature. All diffraction rings could be attributed to ZnO. A decrease in ZnO crystallinity with decreasing bilayer spacing is observed; diffraction rings become diffuse and the grain size reduces. It is interesting to note that with a bilayer spacing of 2.5 nm, the ZnO film became fully amorphous in the nanolaminate (Figure 1(e)). This is probably due to a minimum thickness required to allow crystallization in a thin film.

The mechanical properties were obtained by analysing the load–displacement response of the ALD grown Al_2O_3 and ZnO films as well as their nanolaminates using a Berkovich indenter (see Figure S2 in the supplementary information[20]). The multilayers with smaller bilayer thickness exhibited higher penetration depths at the same load, which suggests that the smaller the bilayer spacing, the softer the entire multilayer. In order to study the nature of this trend of softening, the hardness H and the reduced elastic modulus, E_r, of the nanolaminates were plotted with respect to the bilayer thickness Λ (Figure 2) to obtain the following functional dependencies:

$$H(GPa) = 6.7 \times \Lambda(nm)^{0.1} \qquad (1)$$

$$E_r(GPa) = 140 + 0.27 \times \Lambda(nm) \qquad (2)$$

The functions were found to be independent of the indentation depths used in this study.

The decreasing trend of the reduced elastic modulus of the nanolaminates is attributed to the structural transition from nanocrystalline to amorphous nature of the ZnO interlayers.

The reduction in hardness can be rationalized in the following manner. Since hardness can be directly related to the yield stress σ roughly by a factor of 3,[16] an analogy can be drawn to the classical Hall-Petch strengthening effect $\sigma \sim k \times d^{-0.5}$ found in polycrystalline metals, d being the grain size and k a constant.[17] Reducing the grain size makes operation of dislocation-based deformation mechanisms inside the grain volume increasingly difficult, and the Hall-Petch strengthening effect is observed, $H \sim 1/d^m$.

An *inverse* Hall-Petch like behavior is found for the low-temperature ALD grown ZnO/Al_2O_3 nanolaminates (Eq. (1)). Figure 2 shows that the inverse Hall-Petch like regime extends to a bilayer spacing of about 45 nm, where the average hardness and modulus of the constituent ZnO and Al_2O_3 films is reached. An inverse Hall-Petch relation, $H \sim d^m$, is found in nanocrystalline materials with the exponent m varying from 0.1 to about 1, when the average grain size is below 30 nm.[18] The *reduction* in hardness is attributed to a change in deformation mechanism from dislocation-based to grain boundary sliding, which is the primary deformation mode in nanocrystalline ceramics exhibiting plastic deformation at room temperature and super-plasticity at high temperatures.[19] However, it is important to note that, in this study, softening of the nanolaminates is observed despite the confinement of the nanocrystalline ZnO layers by the amorphous Al_2O_3 layers. Also, noteworthy is the ability to tune the mechanical properties of the nanolaminates below the range of the mechanical properties of the constituent ZnO and Al_2O_3 layers.

In summary, this study has illustrated that nanolaminates of Al_2O_3 and ZnO synthesized by ALD become softer with smaller bilayer spacing due to a structural transition from crystalline to amorphous. The sub-nanometer precision
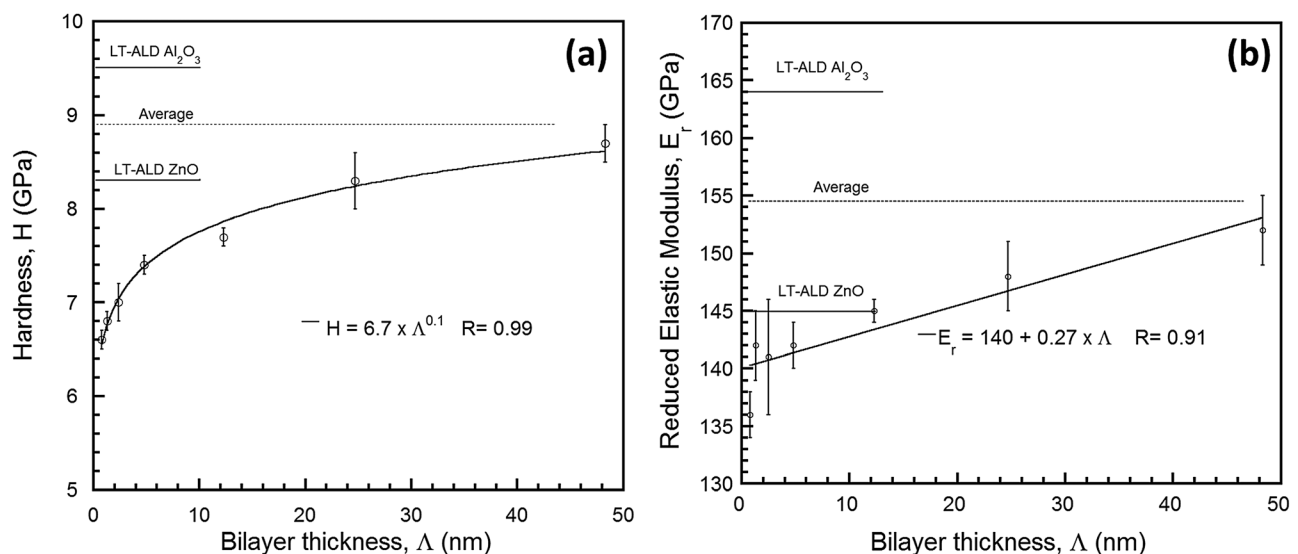

FIG. 2. (a) Hardness (H) and (b) reduced elastic modulus (E_r) versus bilayer thickness (Λ) of the nanolaminates. Values of the low temperature grown (LT-ALD) Al_2O_3 and ZnO films and their average are indicated. Note that the hardness and elastic modulus can be extended below the pure oxide compound values using nanolaminates. R is Pearson's correlation coefficient and a value close to 1 signifies a good quality fit.

control of ALD allows accurate assessment of the mechanical properties of nanocrystalline ceramics with grain sizes within the inverse Hall-Petch regime. The ability to tune the mechanical behavior of thin films via controlling the stacking sequence with the precision of single monolayers by ALD should be very useful in the fields of protective coatings and gas diffusion barriers for photovoltaic devices,[21] window coatings, and food packaging.

[1]S. M. George, Chem. Rev. **110**(1), 111 (2010).

[2]M. Knez, K. Niesch, and L. Niinisto, Adv. Mater. **19**(21), 3425 (2007).

[3]D. M. King, S. I. Johnson, J. H. Li, X. H. Du, X. H. Liang, and A. W. Weimer, Nanotechnology **20**(19), 195401 (2009).

[4]C. Marichy, M. Bechelany, and N. Pinna, Adv. Mater. **24**, 1017 (2012); H. Kim, H. B. R. Lee, and W. J. Maeng, Thin Solid Films **517**(8), 2563 (2009).

[5]M. Knez, A. Kadri, C. Wege, U. Gosele, H. Jeske, and K. Nielsch, Nano Lett. **6**(6), 1172 (2006).

[6]S. M. Lee, E. Pippel, U. Gosele, C. Dresbach, Y. Qin, C. V. Chandran, T. Brauniger, G. Hause, and M. Knez, Science **324**(5926), 488 (2009).

[7]M. D. Groner, F. H. Fabreguette, J. W. Elam, and S. M. George, Chem. Mater. **16**(4), 639 (2004).

[8]V. L. A. Paracchino, K. Sivula, M. Grätzel, and E. Thimsen, Nature Mater. **10**, 456 (2011).

[9]J. Elias, M. Bechelany, I. Utke, R. Erni, D. Hosseini, J. Michler, and L. Philippe, "Urchin-inspired zinc oxide as building blocks for nanostructured solar cells," Nanoscale (Submitted).

[10]D. Bhattacharyya, N. A. Mara, P. Dickerson, R. G. Hoagland, and A. Misra, Philos. Mag. **90**(13), 1711 (2010); K. A. Rzepiejewska-Malyska, W. M. Mook, M. Parlinksa-Wojtan, J. Hejduk, and J. Michler, J. Mater. Res. **24**(3), 1208 (2009); M. A. Phillips, B. M. Clemens, and W. D. Nix,

Acta Mater. **51**(11), 3171 (2003); U. Helmersson, S. Todorova, S. A. Barnett, J. E. Sundgren, L. C. Markert, and J. E. Greene, J. Appl. Phys. **62**(2), 481 (1987); M. Shinn, L. Hultman, and S. A. Barnett, J. Mater. Res. **7**(4), 901 (1992); X. Chu and S. A. Barnett, J. Appl. Phys. **77**(9), 4403 (1995); P. H. Mayrhofer, C. Mitterer, L. Hultman, and H. Clemens, Prog. Mater. Sci. **51**(8), 1032 (2006); S. C. Tjong and H. Chen, Mater. Sci. Eng. R **45**(1–2), 1 (2004); J. S. Koehler, Phys. Rev. B **2**(2), 547 (1970).

[11]S. Veprek and A. S. Argon, Surf. Coat. Technol. **146–147**(0), 175 (2001); S. Veprek, S. Reiprich, and S. H. Li, Appl. Phys. Lett. **66**(20), 2640 (1995).

[12]S. Y. Kuan, X. H. Du, H. S. Chou, and J. C. Huang, Surf. Coat. Technol. **206**(6), 1116 (2011).

[13]H. Cheun, C. Fuentes-Hernandez, J. Shim, Y. Fang, Y. Cai, H. Li, A. K. Sigdel, J. Meyer, J. Maibach, A. Dindar, Y. Zhou, J. J. Berry, J.-L. Bredas, A. Kahn, K. H. Sandhage, and B. Kippelen, Adv. Funct. Mater. **22**(7), 1531 (2012).

[14]Y. Balcaen, N. Radutoiu, J. Alexis, J. D. Beguin, L. Lacroix, D. Samélor, and C. Vahlas, Surf. Coat. Technol. **206**(7), 1684 (2011); R. Katamreddy, R. Inman, G. Jursich, A. Soulet, A. Nicholls, and C. Takoudis, Thin Solid Films **515**(17), 6931 (1986).

[15]J. A. Whitby, F. Oestlund, P. Horvath, M. Gabureac, J. L. Riesterer, I. Utke, M. Hohl, L. Sedlacek, J. Jiruse, V. Friedli, M. Bechelany, and J. Michler, Adv. Mater. Sci. Eng. **2012**,180437.

[16]E. Voce and D. Tabor, J. Inst. Metals **79**(12), 465 (1951).

[17]W. Sylwestrowicz and E. O. Hall, Proc. Phys. Soc. London, Sect. B **64**(378), 495 (1951); N. J. Petch, J. Iron Steel Inst., London **174**(1), 25 (1953).

[18]A. H. Chokshi, A. Rosen, J. Karch, and H. Gleiter, Scr. Metall. **23**(10), 1679 (1989); P. G. Sanders, J. A. Eastman, and J. R. Weertman, Acta Mater. **45**(10), 4019 (1997); E. Arzt, Acta Mater. **46**(16), 5611 (1998); H. Gleiter, Acta Mater. **48**(1), 1 (2000); K. S. Kumar, H. Van Swygenhoven, and S. Suresh, Acta Mater. **51**(19), 5743 (2003).

[19]K. A. Padmanabhan, J. Mater. Sci. **44**(9), 2226 (2009); J. H. Lee, I. Kim, D. M. Hulbert, D. Jiang, A. K. Mukherjee, X. Zhang, and H. Wang, Acta Mater. **58**(14), 4891 (2010).

[20]See supplementary material at http://dx.doi.org/10.1063/1.4711767 for more information about the scanning electron and ion microscopy observations, the indentation experiments, and the experimental section details.

[21]J. Elias, C. Levy-Clement, M. Bechelany, J. Michler, G. Y. Wang, Z. Wang, and L. Philippe, Adv. Mater. **22**(14), 1607 (2010).